Published in final edited form as:
Birth Defects Res A Clin Mol Teratol. 2010 November ; 88(11): 953–964. doi:10.1002/bdra.20719.

Magnetic resonance microscopy-based analyses of the brains of normal and ethanol-exposed fetal mice

Shonagh K. O'Leary-Moore, Ph.D., **Scott E. Parnell, Ph.D.**, **Elizabeth A. Godin, B.S.**, **Deborah B. Dehart, A.S.**, **Jacob J. Ament, B.S.**, **Amber A. Khan, B.S.**, **G. Allan Johnson, Ph.D.**, **Martin A. Styner, Ph.D.**, and **Kathleen K. Sulik, Ph.D.**
Bowles Center for Alcohol Studies (SOM, SEP, EAM, DBD, JJA, AAK, KKS) and Department of Psychiatry (MAS), University of North Carolina, Chapel Hill, NC 27599. Center for *In Vivo* Microscopy, Duke University, Durham NC (GAJ)

Abstract

Background—The application of magnetic resonance microscopy (MRM) to the study of normal and abnormal prenatal mouse development has facilitated discovery of dysmorphology following prenatal ethanol insult. The current analyses extend this work, providing a regional brain volume-based description of normal brain growth and illustrating the consequences of gestational day (GD) 10 ethanol exposure in the fetal mouse.

Methods—To assess normal growth, control C57Bl/6J fetuses collected on GD16, GD16.5, and GD17 were scanned using a 9.4T magnet, resulting in 29μm isotropic resolution images. For the ethanol teratogenicity studies, C57Bl/6J dams were administered ethanol (i.p. @ 2.9 g/kg) at 10 days 0 hr and 10 days 4 hrs post-fertilization and fetuses were collected for analyses on GD17. From individual MR scans, linear measurements and regional brain volumes were determined and compared.

Results—In control fetuses, each of the assessed brain regions increased in volume, while ventricular volumes decreased between GD16 and GD17. Illustrating a global developmental delay, prenatal ethanol exposure resulted in reduced body volumes, crown-rump lengths and a generalized decrease in regional brain volumes as compared to GD17 controls. However, as compared to GD16.5 (morphologically-matched) controls, ethanol exposure resulted in volume increases in the lateral and 3rd ventricles as well as a disproportionate reduction in cortical volume.

Conclusions—The normative data collected herein facilitates the distinction between GD10 ethanol-induced developmental delay and frank dysmorphology. This work illustrates the utility of MRM-based analyses for developmental toxicology studies and extends our knowledge of the stage-dependency of ethanol teratogenesis.

Keywords

Magnetic Resonance Microscopy; Fetal Alcohol Spectrum Disorder; Brain Development; Mouse; Prenatal Ethanol; Ventriculomegaly

Corresponding author: Dr. S.K. O'Leary-Moore, Fetal Toxicology Division, Bowles Center for Alcohol Studies, University of North Carolina at Chapel Hill, CB #7178 Thurston Bowles Building Chapel Hill, NC 27599-7178; (919) 966-3208, somoore@med.unc.edu.
Presented at the 32nd annual meeting of the Research Society on Alcoholism, June 30-July 2, 2009, San Diego, CA.

INTRODUCTION

Recently small animal magnetic resonance imaging methodologies have advanced to a point where rodent anatomy can be visualized at near histological resolution (i.e. approximately 19–40 microns). This high resolution magnetic resonance imaging is now referred to as magnetic resonance microscopy (MRM). Among the advances that have made MRM possible are the availability of high field-strength imaging systems, custom radiofrequency coils, and the application of active-staining contrast agents (eg. Petiet et al, 2007; Petiet et al, 2008; Petiet and Johnson, 2010; Turnbull and Mori, 2007). Of particular use for researchers in the fields of developmental biology, genetics and toxicology is an annotated atlas of prenatal mouse anatomy (Petiet et al, 2008; www.civm.duhs.duke.edu/devatlas/index.html) that was developed employing this technology. Included in this MRM-based atlas are 19.5μm MR scans through gestational day (GD) 10.5 – 19.5 fetal mice.

One of the major utilities of MRM is the ability to accurately define and segment selected anatomical regions from individual scans and to then reconstruct the (isotropic) segmentation data to provide accurate 3-D representations of the images. The morphological and volumetric assessments that this allows are important for appreciating both normal and abnormal development. Illustrating the value of MRM for teratology studies are two recent reports regarding ethanol-induced prenatal brain dysmorphology (Parnell et al, 2009; Godin et al, 2010). These reports describe the defects present in GD17 mouse brains that result from acute ethanol exposure on GD7 and GD8. In addition to brain dysmorphology, other abnormalities were also identified in the ethanol-exposed fetuses. Among these were reductions in total brain and body volume as compared to control animals.

The current study was designed to extend the MRM-bases analyses of developmental stage-dependent prenatal ethanol insult, focusing on identifying the adverse affect of acute GD10 ethanol exposure in mice. Although in mice there is considerable intra-litter variability in developmental stages, early on GD10, mouse embryos of the strain used for this study (C57Bl/6J) typically are at a point in development when the neural tube has just completed its closure, approximately 30–34 pairs of somites are present, and the hind limb buds are becoming morphologically evident (Theiler, 1989). This corresponds to Carnegie stage 13–14 and to 28–32 days post-fertilization in humans. While previous studies have shown that in mice at this stage of embryonic development, selected cell populations within the brain are vulnerable to ethanol-induced cell death (Dunty et al, 2001), the resulting fetal dysmorphology has not been determined.

Realizing the potential of acute GD10 ethanol exposure to yield generalized growth retardation in addition to frank dysmorphology, knowledge of normal growth trajectories as a requirement for distinguishing these end-points was recognized. To this end, MRM was applied to characterization of brain morphology (both form and volume) in GD16, GD16.5 and GD17 control fetuses; i.e. at times preceding and including that at which ethanol-exposed fetuses were similarly examined. Supplementing existing evidence supporting the stage-dependency of fetal alcohol insult, this study holds relevance for Fetal Alcohol Syndrome (FAS) and Fetal Alcohol Spectrum Disorders (FASD), which continue to be diagnosed at alarming rates both in the United States and worldwide (Jones and Smith, 1973; Sokol et al, 2003; May et al, 2009).

MATERIALS & METHODS

Animal Breeding and Maintenance

C57BI/6J mice were purchased from The Jackson Laboratory (Bar Harbor, ME) and were housed in a temperature and light-controlled (12/12 hr light/dark) environment approved by

the Association for Assessment and Accreditation of Laboratory Animal Care. Standard laboratory chow and water was available *ad libitum*. For breeding, 1–2 females were placed with one male for 2 hours. Detection of a copulation plug marked the beginning of gestational day (GD) 0.

Maternal Treatment and Determination of Blood Ethanol Concentrations

On GD10, pregnant mice were randomly assigned to either an ethanol or control group and weighed. The mice in the ethanol group were given an intraperitoneal (ip) dose of 25% ethanol (2.9 g/kg each injection) on GD10 0 hrs and again 4 hrs later. Control dams were administered equivalent doses of Ringer's solution at each of these times. Blood ethanol concentrations (BECs) were determined in a separate group of dams that were administered ethanol on GD10. For this, 30 minutes after the 2nd ethanol injection, 35 μl of blood from a tail clip was collected in a heparinized capillary tube. Whole blood was spun at 3000 rpm for 3 minutes and plasma was frozen and stored at 4 °C overnight. BECs were determined using an ANALOX alcohol analyzer (AM1 Model, Analox Instruments USA Inc., Lunenburg, MA). The average BEC was 424 ± 16 mg/dl. All procedures involving animals were approved by an Institutional Animal Care and Use Committee (IACUC) at the University of North Carolina at Chapel Hill.

Specimen Collection and Preparation for MRM

Following CO_2 anesthesia, groups of control dams on day 16, 16.5 and 17 of their pregnancy, and an ethanol-exposed group on the 17th day were killed by cervical dislocation. Following laparotomy, the uteri were removed and fetuses were dissected free of decidua and placed on ice in phosphate buffered saline (PBS). Fetuses were examined under a dissecting microscope for any gross abnormalities. For MRM analyses, selection of the ethanol-exposed fetuses was based on the presence of grossly-observable dysmorphology (especially the presence of ocular anomalies and/or limb defects), an approach that is comparable to selection of children with known physical features of FAS for subsequent study. Ocular defects among ethanol-exposed subjects ranged from slight microphthalmia to coloboma. For each of the 3 control groups, specimens representative of the litters (based primarily on fetal size) were selected. A total of 9 GD17 ethanol-exposed fetuses from 5 litters, as well as, 6 GD16, 5 GD16.5, and 6 GD17 control fetuses from 10 litters were selected. These fetuses were photographed to document size and any gross anomalies and then processed for imaging. For this, the fetuses were drop fixed in a 20:1 solution of Bouin's fixative (Sigma-Aldrich, St. Louis, MO) and Prohance (Bracco Diagnostics Inc. Princeton, NJ) for 9 hours (Petiet et al, 2007; Petiet & Johnson, 2010). This was followed by a brief PBS rinse and placement in a storage solution containing 200:1 PBS:Prohance. Fetuses were typically imaged within 72 hrs of fixation.

MRM

MRM was conducted at the Duke Center for *In Vivo* Microscopy using an Oxford 9.4T/8.9 cm bore magnet interfaced with a GE EXCITE console (Epic 12.0). Fetuses were placed into acrylic holders and immersed in fomblin, a perfluorocarbon that limits dehydration of the sample and reduces scanning susceptibility artifacts. Images were acquired in a 20 mm diameter solenoid radiofrequency coil using a RF refocused spin echo sequence (TR = 75 ms, TE = 5.228 ms). Asymmetric partial Fourier sampling (Johnson et al, 2007) into a 512 × 512 × 1024 array resulted in Nyquist limited spatial resolution of 29 μm (voxel volumes of approximately 25 pL). Scanning time totaled approximately 4 hours for each fetus.

Histological analysis

After MRM scanning was completed, subjects were stored in 70% ethanol until embedded in paraffin for histological analyses. Sections were cut at a 10 μm slice thickness, mounted on slides and stained using a routine aqueous hematoxylin and eosin (H&E) staining protocol.

Volumetric Segmentation and Measurements

For segmentation and volumetric analyses, ITK-SNAP, a software program originally developed at the University of North Carolina, Chapel Hill (Yushkevich et al 2006), was utilized. Before segmentation, each brain was realigned and straightened using ImageJ (version 1.38 NIH; www.rsbweb.nih.gov/ij) in order to ensure optimal accuracy during segmentation. Using the automatic segmentation tool in ITK-SNAP, total body volumes were computed for each subject. Regional brain volumes for each subject were determined from manual tracings. The regions assessed were: cerebral cortices, olfactory bulbs, hippocampus, striatum, septal region, diencephalon, mesencephalon, pons & medulla, cerebellum, pituitary gland, lateral ventricles, 3rd ventricle, and mesencephalic and 4th ventricle (see figure 1). Brain tracings were made by 3 individuals trained in fetal mouse brain anatomy (SOM, JJA, AAK), with regions traced by each person being consistent for all animals. Intra-rater reliability was assessed by calculating a coefficient of variation and averaged 3% for all brain regions (range 0.1% – 11%). Regional boundaries were based on existing mouse embryo atlases (Kaufman, 1992; Schambra 2008; Schambra et al, 1992). Voxel counts were generated within ITK-SNAP for each region and volume measurements were made for each animal by multiplying the number of voxels for each region by the volume of a voxel (25 pL). Total brain volume was determined by summation of all of the volumes of the individual brain regions.

Linear Measurements

In addition to volumetric assessments, linear measurements were determined for each subject using Image J (figure 2). The following measures were acquired at the three different levels of the brain shown in figure 2a: transverse cerebellar diameter (figure 2b), midsagittal brain length, frontothalamic distance, brain width, septal region width, olfactory bulb length and width, 3rd ventricle width, diencephalon length and width (figure 2c), and pituitary length and width (figure 2d).

Statistical Analyses

For analyses of normal brain development, both linear measurements and regional brain volume changes were assessed using Multivariate Analyses of Variance (MANOVA) with 1 independent variable (Age) consisting of 3 levels (GD16 controls, GD16.5 controls, GD17 controls). Student-Newman Keuls (SNK) *post hoc* tests were conducted to follow up significant MANOVAs when necessary. Analysis of developmental and ethanol-induced changes in growth parameters, specifically crown-rump length, total body volume and total brain volume, were conducted using ANOVAs consisting of 4 levels (GD16 controls, GD16.5 controls, GD17 controls and GD17 prenatal ethanol exposed). The identification of a morphologically-matched group of controls was accomplished with these analyses and SNK *post hoc* tests. Subsequent evaluation of the prenatal ethanol-exposed group was conducted using the GD16.5 controls as the group that was deemed to be the best suited as a morphologically-matched control group. Additionally, in order to ascertain any disproportionate effects of ethanol exposure on the brain, the ratio of each brain region to the overall brain volume was computed for each subject and analyzed using separate MANOVAs. This approach is similar to the statistical analysis in a previous MRM-based report (Parnell et al, 2009). An alpha value of 0.05 was maintained for all analyses.

RESULTS

Control Morphological and Volumetric Data

As illustrated in 3D MRM reconstructions, in control fetuses notable changes in brain size and morphology occur between GD16 and GD17 (figure 3). In addition to an overall size increase, as development progresses the postero-lateral aspects of the cerebral cortical hemispheres extend further caudally, covering more of the diencephalon. Particularly obvious is the changing morphology of the olfactory bulbs, which become relatively elongated, and of the 3rd ventricle, which becomes narrower, especially in its dorsal portion. In addition, MRM-based analyses made it possible to readily determine total body, brain and regional tissue volumes. For the former, between GD16 and GD17 body volume increased by 71%, while brain size increased approximately 38% (figure 4). CRL also increased by 16% from GD16 to GD17 (figure 4).

Developmental changes in regional brain volume determinations are consistent with visual inspection of the 3D reconstructions (table 1). Indeed, a significant effect of age was apparent for the MANOVA on raw volumetric data (Wilks' Lambda = 0.015; ($F(20,10) = 3.575$, $p < 0.05$) and examination of the between subject effects revealed significant differences between groups for every regional brain volume assessed (all p's < 0.05). From GD16 to GD17, the following control regional brain volume increases occurred: cerebral cortices, 42%; diencephalon, 41%; olfactory bulbs, 103%; striatum, 60%; hippocampus, 67%; septal region, 53%; mesencephalon, 40%; pons & medulla, 41%; cerebellum, 39% (all p's < 0.05; see table 1). Post-hoc tests indicated that for the cerebral cortices, diencephalon, olfactory bulbs, striatum, midbrain, and pons & medulla, volumes were significantly smaller in the GD16 controls as compared to both GD16.5 and GD17 controls and GD16.5 controls had significantly smaller volumes as compared to GD17 controls (all p's < 0.05). Further, although significantly smaller than the GD17 controls, volumes of the hippocampus, cerebellum and pituitary did not differ between GD16 and GD16.5 controls (all p's < 0.05; table 1).

In addition to the brain tissue, a MANOVA analyzing developmental trends in ventricular space was also found to be significant (Wilk's lambda = 0.19; $F(3,6) = 5.184$, $p < 0.05$). Specifically, the volumes of the 3rd ventricle and mesencephalic & 4th ventricle decreased significantly (3rd: 43%; mesencephalic & 4th: 16%) between GD16 and GD17 (3rd: $F(2,14) = 19.29$, $p < 0.05$; mesencephalic & 4th: $F(2,14) = 5.73$ $p < 0.05$). Post hoc tests revealed that volumes of the 3rd and mesencephalic & 4th ventricles did not differ between GD17 and GD16.5 controls but that they were both significantly smaller as compared to the GD16 controls (p's < 0.05; table 1). No significant developmental changes in the volumes of the lateral ventricles were notable between GD16 and GD17.

Volumetric Data for Ethanol-Exposed Fetuses

Examination of total body volume and crown rump length (CRL) data revealed that for the ethanol-exposed subjects, these measures were significantly smaller than for the chronologically-matched GD17 controls (total body: ($F(3,22) = 11.672$, $p < 0.01$); CRL: ($F(3,22) = 7.301$, $p < 0.01$), SNK *post hoc* tests, p's < 0.05; figure 4). Overall, the body size of the GD16.5 control group was most comparable to that of the GD17 ethanol-exposed group. Total brain volume data (mm^3) was consistent with this trend, with brain volume in the ethanol-exposed group being significantly smaller than that of the GD17 controls' but also significantly larger than that of the GD16 controls' ($F(3, 22) = 16.85$, $p < 0.01$; figure 4). Likewise, comparisons between the GD17 controls and the prenatal ethanol-exposed subjects on raw volumetric data indicated a generalized reduction in regional brain volumes in the latter (see table 1). Together, these data provided the basis for considering the GD16.5

fetuses as the most morphologically-comparable control group against which to compare the effects of prenatal ethanol exposure.

In regards to regional changes in raw brain and ventricular volumes, when comparing the prenatal ethanol exposed group with their morphologically matched control counterparts, significant ethanol effects were evident (ventricles: Wilk's lambda = 0.23; $F(3,10) = 8.705$, $p < 0.01$; brain tissue: Wilk's lambda = 0.023; $F(10,3) = 0.03$, $p < 0.05$). Specifically, as shown in table 1, the volumes of the lateral and 3rd ventricles as well as the pituitary volume were significantly increased following the ethanol insult (lateral ventricles: $F(1,12) = 15.71$, $p < 0.01$; 3rd ventricle: $F(1.12) = 9.582$, $p < 0.01$; pituitary: $F(1,12) = 8.261$, $p < 0.05$). Similarly, a trend toward an increase in mesencephalic & 4th ventricular volume was evident but failed to reach statistical significance ($p = 0.053$).

In addition to examining the raw volumetric data for ethanol-induced alterations in brain and ventricular volumes, as in the Parnell et al, (2009) MRM study, in order to ascertain any disproportionate effects of ethanol exposure, each regional brain measurement was analyzed as a percentage of total brain volume. Because the GD16.5 controls were morphologically best-matched to the GD17 ethanol-exposed fetuses (see figure 4), only the comparisons between this control group and the ethanol-exposed group are illustrated (figure 5). Significant MANOVAs revealed that group differences existed for both ventricular volumes and regional brain tissue volumes (ventricles: Wilk's lambda = 0.389; $F(3,10) = 5.231$, $p < 0.05$; brain: Wilk's lambda = 0.03; $F(10,3) = 9.604$, $p < 0.05$). Specifically, prenatal ethanol exposure significantly reduced the standardized volume of the cerebral cortex ($F(1,12) = 8.029$, $p < 0.05$). In contrast, prenatal ethanol exposure increased the volume of the diencephalon ($F(1,12) = 8.372$, $p < 0.05$) as compared to morphologically-matched controls. A significant increase in the proportion of 3rd ventricular volume to brain volume after prenatal ethanol-exposure was also evident ($F(1,12) = 5.95$, $p < 0.01$) (figure 5). Although not statistically significant, lateral and mesencephalic & 4th ventricular volumes were increased 14% and 13%, respectively, following prenatal ethanol exposure as compared to the GD16.5 controls.

Linear Measurements

Consistent with volumetric analyses, a MANOVA also revealed significant differences in linear measurements among the 3 groups of control fetuses (Wilk's lambda = 0.002; $F(24,8) = 6.070$, $p < 0.05$; table 2). Tests of between group effects indicated significant age-related changes for the following: brain length, cortical brain width, frontothalamic distance, transverse cerebellar diameter, olfactory bulb length and width, septal region width, diencephalon length and width, pituitary length and width and 3rd ventricle width (all p's < 0.05) (table 2). Although the overall MANOVA comparing the morphologically matched controls with the prenatal ethanol-exposed animals was not significant, consistent with the volumetric data, in the between subject group analysis, 3rd ventricle width was significantly larger in the ethanol-exposed subjects as compared to the GD16.5 controls' ($F(1,12) = . 10.389$; $p < 0.05$). Other significant differences in linear measurements between prenatal ethanol-exposed and morphologically matched controls were evident in pituitary length and septal region width ($F(1, 12) = 11.33$, $p < 0.05$; $F(1,12) = 11.79$, $p < 0.05$) (table 2).

Dysmorphology

In addition to volumetric and linear alterations, considerable dysmorphology was evident among the ethanol-exposed fetuses. The abnormal form of the ventricles was particularly notable. Figure 6 illustrates the ventricular dysmorphology that was present in 6 of the 9 ethanol-exposed fetuses examined (figure 6b–g). The abnormal shape of the 3rd ventricle is especially apparent, with variable expansion both dorsally (arrows) and ventrally

(arrowheads) in the space surrounded by the diencephalon. In addition, the mesencephalic ventricular space (cerebral aqueduct) is notably enlarged in some specimens (e.g. figure 6g, dashed arrow). H & E-stained histological sections (figure 7) and individual MRM scans (figure 8) confirmed these findings.

Also well-illustrated by the MRM scans, and consistent with volumetric assessments, is ethanol-induced cerebral cortical deficiency (figure 8). Comparison of the images from the 2 ethanol-exposed fetuses to that of a GD16.5 control illustrates reduced thickness of the cerebral cortices accompanied by lateral ventricular dilation in the affected specimens. As previously noted, the degree of effect is variable between subjects.

In addition to the cortical alterations and ventricular dysmorphology that resulted from the GD10 ethanol exposure, MRM revealed a heterotopic mass in the hypothalamic region of the mildly dilated 3rd ventricle of one ethanol-exposed subject (figure 9a and b). Otherwise, the appearance of the brain and ventricles of this animal was generally consistent with that of other ethanol-exposed subjects. Subsequent to MRM imaging, routine histological analysis confirmed this finding (figure 9c and d). Although, in one histological section, the mass appeared to be unattached (figure 9c), another section (figure 9d) illustrates where the heterotopia extends from the hypothalamus. The aberrant mass is histologically similar to that of the surrounding neural tissue.

DISCUSSION

This work illustrates the fetal brain dysmorphology that results from acute GD10 ethanol exposure in mice and the utility of MRM-based methodologies for this type of investigation. In particular, regional brain segmentation and 3-D reconstruction have allowed assessment of volumetric as well as morphological alterations. In distinguishing ethanol-induced dysmorphology from generalized developmental delay, normal regional brain growth trajectories as established from MRM data have been especially valuable. As expected regarding the latter, raw volumetric data from GD16, GD16.5 and GD17 fetal brains showed age-related increases for the entire brain and for each of its sub-regions that were analyzed. Notably, the overall 38% brain volume increase that occurred between GD16 and GD17 was accompanied by a 16% reduction in the total ventricular volume, with the reduction in the volume of the 3rd ventricle over this period of time being particularly pronounced. In comparing GD17 ethanol-exposed fetuses to controls, the GD16.5 control group was found to be developmentally most comparable; i.e. the ethanol-exposed fetuses were delayed in their development by about a half day. Importantly however, compared to the GD16.5 control group, prenatal ethanol exposure significantly increased both the lateral and 3rd ventricular volumes; volumes that should be decreasing with time. In addition to the volumetric changes, the morphology of the 3rd ventricle following GD10 maternal ethanol treatment was abnormal as compared to that in all control stages examined.

Ventricular enlargement has also been noted in other FASD models (eg. Mattson et al, 1994; Sakata-Haga et al, 2004; Zhou et al, 2003) as well as in clinical studies of prenatal alcohol exposure (Johnson et al, 1996; Swayze et al, 1997). In humans, ventriculomegaly can be diagnosed prenatally and is associated with subsequent developmental delays and a high risk of other types of brain anomalies including lissencephaly, absent corpus callosum, septo-optic dysplasia, hydrocephalus and aqueductal stenosis (reviewed by Laskin et al, 2005; Gaglioti et al, 2009). Of these, agenesis of the corpus callosum is the most frequently detected co-occurring anomaly (Griffiths et al, 2010). In fetuses with prenatally-diagnosed ventriculomegaly, further prenatal examination with MR is, therefore, indicated (Manfredi et al, 2009). Based on the current findings, additionally indicated is acquisition of maternal drinking history.

In addition to ventricular changes, regional brain abnormalities were also noted among the ethanol-exposed fetuses that were examined. In particular, the volume of the cerebral cortex was found to be reduced. While exposure paradigms have varied, several studies in animal models have shown that the cerebral cortex is especially sensitive to gestational ethanol exposure (eg. Miller & Potempa, 1990; Mihalick et al, 2001, Burke et al, 2009; Godin et al, 2010). Human MRI data has also indicated that ethanol exposure during gestation has a disproportionate effect on the developing cerebral cortex (reviewed by Spadoni et al, 2007; Norman et al, 2009). An over-abundance of gray matter and not enough white matter in cortical regions around the left posterior parietal cortex has been reported in prenatally ethanol-exposed individuals (Sowell et al, 2001). Additionally, alterations in gray matter asymmetry in the posterior/inferior temporal lobe regions (Sowell et al, 2002), as well as an excess in cortical thickness in bilateral temporal, inferior parietal and frontal regions (Sowell et al, 2008) have been found. Further examination utilizing sophisticated image analyses tools in animal models could provide additional insight as to subregions of the cortex that are especially sensitive to specific ethanol exposure periods.

That the 3rd ventricle was enlarged and dysmorphic in a large proportion of the ethanol-exposed fetuses examined may be suggestive of insult to the surrounding brain tissue; the diencephalon/thalamus and hypothalamus. However, thalamic volumes were unchanged in the analysis of raw volume data and actually increased when taking into account total brain size following prenatal ethanol exposure. The latter is likely explained by the substantial decrease in cortical volumes after prenatal ethanol exposure. In regard to the former, given the limited size of the 3rd ventricle, even a small increase in the number of voxels translates to a large change in the overall 3rd ventricular volume. A reduction of this same magnitude in a large region such as the thalamus would not necessarily result in any statistically identified result. More detailed examination and segmentation of sub-regions of the thalamus and hypothalamus could potentially uncover volume deficits. Supporting this expectation is a previous report by Dunty and colleagues (2001) who examined patterns of cell death following acute ethanol exposure at varying time points and found that the hypothalamus was particularly affected following acute ethanol exposure on GD10.5 (Dunty et al, 2001). As discussed in a review by Weinberg et al, (2008), that alterations in the hypothalamic-pituitary-adrenal (HPA) axis can be induced following maternal administration of an ethanol-containing liquid diet throughout pregnancy is a well-established finding. Additionally, Park et al, (2004) showed that in C57Bl/6J mice, acute early gestational exposure to ethanol enhances a corticosterone-mediated response to stress. Clearly, along with more detailed histological analyses, postnatal functional analyses with particular attention to perturbations of hormonal cascades are needed as a follow up to the current observations.

The finding in this study of a periventricular heterotopias extending into the 3rd ventricular space of one of the ethanol-exposed fetuses also illustrates insult to the diencephalon. A similar 3rd ventricle heterotopias was previously reported to result from acute ethanol exposure on GD7 in mice (Sulik et al, 1984). In a previous MRM-based study, acute GD7 ethanol exposure was shown to cause (leptomeningeal) cerebral cortical heterotopias in mice (Godin et al, 2010) and both cortical heterotopias and heterotopias localized to the lateral ventricle and interventricular foramen after gestational ethanol exposure have been reported in rats (Komatsu et al, 2001; Sakata-Haga et al, 2004). Both cerebral cortical heterotopias and ventricular heterotopias have been found in humans exposed to ethanol during gestation (eg. Jones & Smith, 1973; Coulter et al, 1993; Clarren et al, 1978; Peiffer et al, 1979; Clarren et al, 1981). Heterotopias are highly linked to seizure activity (Verrotti et al, 2009). Given the heightened prevalence of seizure activity among individuals with prenatal alcohol exposure as compared to the general population (eg. Sun et al, 2009, Bell et al, 2010), and considering the occurrence of low seizure thresholds in FASD rodent models (Bonthius et

al, 2001a; Bonthius et al, 2001b), it is likely that as imaging technologies advance more heterotopias will be discovered in both humans and animal models. Indeed, a very recent case report describes MRI-based discovery of polymicrogyria and two periventricular lesions in a 16 year old girl with FAS who presented with seizures (Reinhardt et al, 2010).

As compared to the MRM-based findings reported for acute ethanol-induced GD7 and GD8 fetal brain changes (Parnell et al, 2009; Godin et al, 2010), the GD10 pattern of insult differs. The holoprosencephaly spectrum characterizes the GD7 ethanol exposure time, but did not result from GD10 treatment. Notable following GD8 insult was a reduction in hippocampal, olfactory bulb, and cerebellar volumes in which the right side of the brain tended to be preferentially affected, a finding not evident in the current study (Parnell et al, 2009). Further, GD8 treatment increased 4th ventricular volume, while GD10 treatment has a major affect on the 3rd ventricle. Analyses of data from other days of acute ethanol insult to the mouse embryo (esp. GD9 & GD11) are currently being finalized, with preliminary results indicating unique dysmorphology patterns for each (unpublished observations).

Despite its limitations (e.g. cost, scanning time, access to sophisticated imaging systems), MRM affords unprecedented opportunities to define teratogenic endpoints. In addition to examination of brain dysmorphology as described herein, the application of MRM to the study of other organ systems holds significant promise. To date, MRM-based studies of normal and abnormal cardiovascular system development have proven particularly informative (Smith, 2001; Petiet et al, 2008), further highlighting the potential of this technology for teratology investigations. Although MRM cannot replace standard teratological techniques such as routine histology and Wilson's razor sections, with advancing technology that will enable more rapid imaging and lower costs for each specimen, and with more imaging centers becoming available, undoubtedly, MRM will be more widely employed to assess whole body morphology.

In conclusion, recognition that GD10 ethanol exposure in mice yields not only growth retardation, but a stage-dependent pattern of CNS defects was facilitated by the generation of, and comparison to, MRM-based data illustrating normal regional brain growth trajectories. A major effect on ventricular and cortical volume was shown. Clinical application of these findings rests, in part, in appreciation of the fact that these defects can arise from insult at a period in development corresponding to times prior to the middle of the first human trimester and the potential of even early human prenatal imaging to identify these types of CNS changes (eg. Kfir et al, 2009).

Acknowledgments

Sources of Support: This work was supported by NIH/NIAAA grants AA007573, P60 AA011605, U01 AA017124; NCRR/NCI grants P41 05959 and U24 CA092656; and the UNC Neurodevelopmental Disorders Research Center HD 03110; and was conducted in conjunction with the Collaborative Initiative on Fetal Alcohol Spectrum Disorders (CIFASD). Additional information about the CIFASD can be found at www.cifasd.org.

Literature Cited

Bell SH, Stade B, Reynolds JN, Rasmussen C, Andrew G, Hwang PA, Carlen PL. The Remarkably High Prevalence of Epilepsy and Seizure History in Fetal Alcohol Spectrum Disorders. Alcohol Clin Exp Res.

Bonthius DJ, Pantazis NJ, Karacay B, Bonthius NE, Taggard Da, Lothman EW. Alcohol exposure during the brain growth spurt promotes hippocampal seizures, rapid kindling, and spreading depression. Alcohol Clin Exp Res. 2001; 25(5):734–745. [PubMed: 11371723]

Bonthius DJ, Woodhouse J, Bonthius NE, Taggard DA, Lothman EW. Reduced seizure threshold and hippocampal cell loss in rats exposed to alcohol during the brain growth spurt. Alcohol Clin Exp Res. 2001; 25(1):70–82. [PubMed: 11198717]

Burke MW, Palmour RM, Ervin FR, Ptito M. Neuronal reduction in frontal cortex of primates after prenatal alcohol exposure. Neuroreport. 2009; 20(1):13–17. [PubMed: 18987558]

Clarren SK. Recognition of fetal alcohol syndrome. JAMA. 1981; 245(23):2436–2439. [PubMed: 7230482]

Clarren SK, Alvord EC Jr, Sumi SM, Streissguth AP, Smith DW. Brain malformations related to prenatal exposure to ethanol. J Pediatr. 1978; 92(1):64–67. [PubMed: 619080]

Coulter CL, Leech RW, Schaefer GB, Scheithauer BW, Brumback RA. Midline cerebral dysgenesis, dysfunction of the hypothalamic-pituitary axis, and fetal alcohol effects. Arch Neurol. 1993; 50(7): 771–775. [PubMed: 8323485]

Dunty WC Jr, Chen SY, Zucker RM, Dehart DB, Sulik KK. Selective vulnerability of embryonic cell populations to ethanol-induced apoptosis: implications for alcohol-related birth defects and neurodevelopmental disorder. Alcohol Clin Exp Res. 2001; 25(10):1523–1535. [PubMed: 11696674]

Gaglioti P, Oberto M, Todros T. The significance of fetal ventriculomegaly: etiology, short- and long-term outcomes. Prenat Diagn. 2009; 29(4):381–388. [PubMed: 19184972]

Godin EA, O'Leary-Moore SK, Khan AA, Parnell SE, Ament JJ, Dehart DB, Johnson BW, Allan Johnson G, Styner MA, Sulik KK. Magnetic resonance microscopy defines ethanol-induced brain abnormalities in prenatal mice: effects of acute insult on gestational day 7. Alcohol Clin Exp Res. 34(1):98–111. [PubMed: 19860813]

Griffiths PD, Reeves MJ, Morris JE, Mason G, Russell SA, Paley MN, Whitby EH. A prospective study of fetuses with isolated ventriculomegaly investigated by antenatal sonography and in utero MR imaging. AJNR Am J Neuroradiol. 31(1):106–111. [PubMed: 19762458]

Johnson GA, Ali-Sharief A, Badea A, Brandenburg J, Cofer G, Fubara B, Gewalt S, Hedlund LW, Upchurch L. High-throughput morphologic phenotyping of the mouse brain with magnetic resonance histology. Neuroimage. 2007; 37(1):82–89. [PubMed: 17574443]

Johnson VP, Swayze VW II, Sato Y, Andreasen NC. Fetal alcohol syndrome: craniofacial and central nervous system manifestations. Am J Med Genet. 1996; 61(4):329–339. [PubMed: 8834044]

Jones KL, Smith DW. Recognition of the fetal alcohol syndrome in early infancy. Lancet. 1973; 302(7836):999–1001. [PubMed: 4127281]

Kaufman, MH. The Atlas of Mouse Development. San Diego: Academic Press; 1992.

Kfir M, Yevtushok L, Onishchenko S, Wertelecki W, Bakhireva L, Chambers CD, Jones KL, Hull AD. Can prenatal ultrasound detect the effects of in-utero alcohol exposure? A pilot study. Ultrasound Obstet Gynecol. 2009; 33(6):683–689. [PubMed: 19444822]

Komatsu S, Sakata-Haga H, Sawada K, Hisano S, Fukui Y. Prenatal exposure to ethanol induces leptomeningeal heterotopia in the cerebral cortex of the rat fetus. Acta Neuropathol. 2001; 101(1): 22–26. [PubMed: 11194937]

Laskin MD, Kingdom J, Toi A, Chitayat D, Ohlsson A. Perinatal and neurodevelopmental outcome with isolated fetal ventriculomegaly: a systematic review. J Matern Fetal Neonatal Med. 2005; 18(5):289–298. [PubMed: 16390787]

Manfredi R, Tognolini A, Bruno C, Raffaelli R, Franchi M, Pozzi Mucelli R. Agenesis of the corpus callosum in fetuses with mild ventriculomegaly: role of MR imaging. Radiol Med. 115(2):301–312. [PubMed: 20017009]

Mattson SN, Riley EP, Jernigan TL, Garcia A, Kaneko WM, Ehlers CL, Jones KL. A decrease in the size of the basal ganglia following prenatal alcohol exposure: a preliminary report. Neurotoxicol Teratol. 1994; 16(3):283–289. [PubMed: 7935262]

May PA, Gossage JP, Kalberg WO, Robinson LK, Buckley D, Manning M, Hoyme HE. Prevalence and epidemiologic characteristics of FASD from various research methods with an emphasis on recent in-school studies. Dev Disabil Res Rev. 2009; 15(3):176–192. [PubMed: 19731384]

Mihalick SM, Crandall JE, Langlois JC, Krienke JD, Dube WV. Prenatal ethanol exposure, generalized learning impairment, and medial prefrontal cortical deficits in rats. Neurotoxicol Teratol. 2001; 23(5):453–462. [PubMed: 11711248]

Miller MW, Potempa G. Numbers of neurons and glia in mature rat somatosensory cortex: effects of prenatal exposure to ethanol. J Comp Neurol. 1990; 293(1):92–102. [PubMed: 2312794]

Norman AL, Crocker N, Mattson SN, Riley EP. Neuroimaging and fetal alcohol spectrum disorders. Dev Disabil Res Rev. 2009; 15(3):209–217. [PubMed: 19731391]

Park E, Dumas R, Schuller-Levis G, Rabe A. Exposure to alcohol on E9 raises poststress corticosterone in mature but not old mice. Neurosci Lett. 2004; 368(3):345–348. [PubMed: 15364425]

Parnell SE, O'Leary-Moore SK, Godin EA, Dehart DB, Johnson BW, Allan Johnson G, Styner MA, Sulik KK. Magnetic resonance microscopy defines ethanol-induced brain abnormalities in prenatal mice: effects of acute insult on gestational day 8. Alcohol Clin Exp Res. 2009; 33(6):1001–1011. [PubMed: 19302087]

Peiffer J, Majewski F, Fischbach H, Bierich JR, Volk B. Alcohol embryo-and fetopathy. Neuropathology of 3 children and 3 fetuses. J Neurol Sci. 1979; 41(2):125–137. [PubMed: 438847]

Petiet A, Hedlund L, Johnson GA. Staining methods for magnetic resonance microscopy of the rat fetus. J Magn Reson Imaging. 2007; 25(6):1192–1198. [PubMed: 17520739]

Petiet A, Johnson GA. Active staining of mouse embryos for magnetic resonance microscopy. Methods Mol Biol. 611:141–149. [PubMed: 19960328]

Petiet AE, Kaufman MH, Goddeeris MM, Brandenburg J, Elmore SA, Johnson GA. High-resolution magnetic resonance histology of the embryonic and neonatal mouse: a 4D atlas and morphologic database. Proc Natl Acad Sci U S A. 2008; 105(34):12331–12336. [PubMed: 18713865]

Reinhardt K, Mohr A, Gartner J, Spohr HL, Brockmann K. Polymicrogyria in fetal alcohol syndrome. Birth Defects Res A Clin Mol Teratol. 88(2):128–131. [PubMed: 19764076]

Sakata-Haga H, Sawada K, Ohnishi T, Fukui Y. Hydrocephalus following prenatal exposure to ethanol. Acta Neuropathol. 2004; 108(5):393–398. [PubMed: 15365720]

Schambra, UB. Prenatal Mouse Brain Atlas. New York: Springer Science + Business Media; 2008.

Schambra, UB.; Lauder, JM.; Silver, K. Atlas of Prenatal Mouse Brain. San Diego: Academic Press; 1992.

Smith BR. Magnetic Resonance Microscopy in Cardiac Development. Microsc Res Tech. 2001; 52(3): 323–300. [PubMed: 11180623]

Sokol RJ, Delaney-Black V, Nordstrom B. Fetal alcohol spectrum disorder. JAMA. 2003; 290(22): 2996–2999. [PubMed: 14665662]

Sowell ER, Mattson SN, Kan E, Thompson PM, Riley EP, Toga AW. Abnormal cortical thickness and brain-behavior correlation patterns in individuals with heavy prenatal alcohol exposure. Cereb Cortex. 2008; 18(1):136–144. [PubMed: 17443018]

Sowell ER, Thompson PM, Mattson SN, Tessner KD, Jernigan TL, Riley EP, Toga AW. Voxel-based morphometric analyses of the brain in children and adolescents prenatally exposed to alcohol. Neuroreport. 2001; 12(3):515–523. [PubMed: 11234756]

Sowell ER, Thompson PM, Peterson BS, Mattson SN, Welcome SE, Henkenius AL, Riley EP, Jernigan TL, Toga AW. Mapping cortical gray matter asymmetry patterns in adolescents with heavy prenatal alcohol exposure. Neuroimage. 2002; 17(4):1807–1819. [PubMed: 12498754]

Spadoni AD, McGee CL, Fryer SL, Riley EP. Neuroimaging and fetal alcohol spectrum disorders. Neurosci Biobehav Rev. 2007; 31(2):239–245. [PubMed: 17097730]

Sulik KK, Lauder JM, Dehart DB. Brain malformations in prenatal mice following acute maternal ethanol adminstration. Int J Dev Neurosci. 1984; 2(3):203–214.

Sun Y, Strandberg-Larsen K, Vestergaard M, Christensen J, Nybo Andersen AM, Gronbaek M, Olsen J. Binge drinking during pregnancy and risk of seizures in childhood: a study based on the Danish National Birth Cohort. Am J Epidemiol. 2009; 169(3):313–322. [PubMed: 19064645]

Swayze VW 2nd, Johnson VP, Hanson JW, Piven J, Sato Y, Giedd JN, Mosnik D, Andreasen NC. Magnetic resonance imaging of brain anomalies in fetal alcohol syndrome. Pediatrics. 1997; 99(2): 232–240. [PubMed: 9024452]

Theiler, K. The House Mouse: Atlas of Embryonic Development. New York: Springer-Verlag; 1989.

Turnbull DH, Mori S. MRI in mouse developmental biology. NMR Biomed. 2007; 20(3):265–274. [PubMed: 17451170]

Verrotti A, Spalice A, Ursitti F, Papetti L, Mariani R, Castronovo A, Mastrangelo M, Iannetti P. New trends in neuronal migration disorders. Eur J Paediatr Neurol. 14(1):1–12. [PubMed: 19264520]

Weinberg J, Sliwowska JH, Lan N, Hellemans KG. Prenatal alcohol exposure: foetal programming, the hypothalamic-pituitary-adrenal axis and sex differences in outcome. J Neuroendocrinol. 2008; 20(4):470–488. [PubMed: 18266938]

Yushkevich PA, Piven J, Hazlett HC, Smith RG, Ho S, Gee JC, Gerig G. User-guided 3D active contour segmentation of anatomical structures: significantly improved efficiency and reliability. Neuroimage. 2006; 31(3):1116–1128. [PubMed: 16545965]

Zhou FC, Sari Y, Powrozek T, Goodlett CR, Li TK. Moderate alcohol exposure compromises neural tube midline development in prenatal brain. Brain Res Dev Brain Res. 2003; 144(1):43–55.

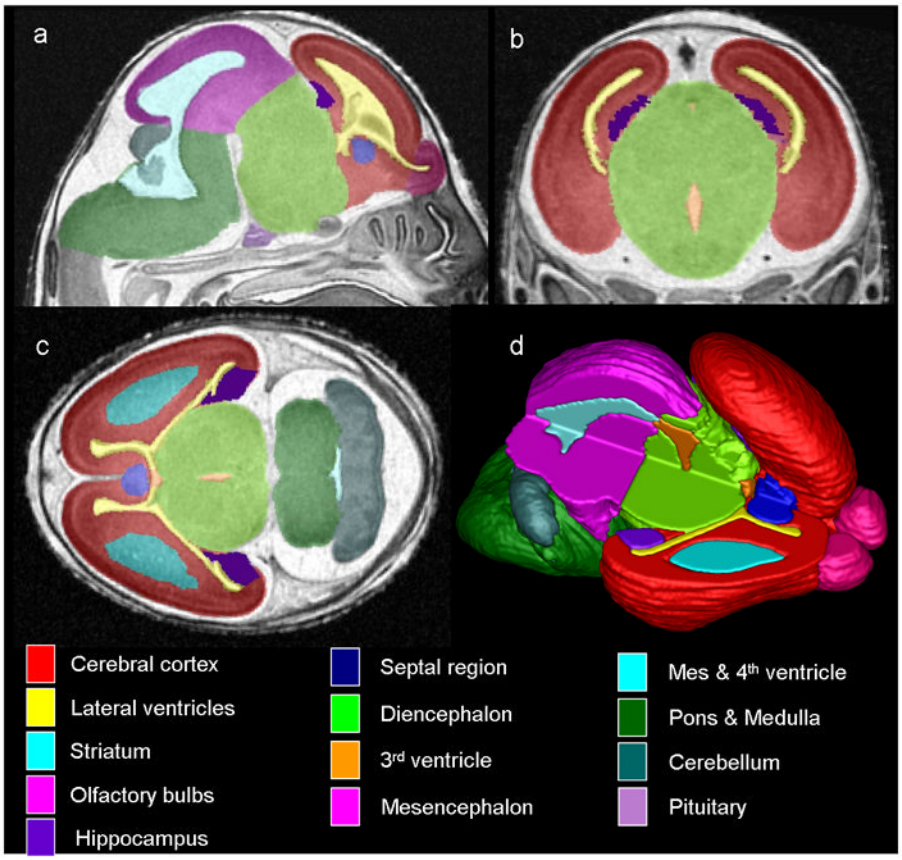

Figure 1.
MRM scans of GD17 fetuses allow for assessment of the brain in 3 planes simultaneously (a - sagittal, b – coronal, c –horizontal), as well as for the creation of 3D reconstructions (d). Color-coded regions illustrate brain areas that were manually segmented for volumetric analyses. Color-codes are listed below (not shown is the pituitary). In d, the upper right portion of the brain image was removed to allow for visualization of the interior structures (modified from Parnell et al, 2009; Godin et al, 2010).

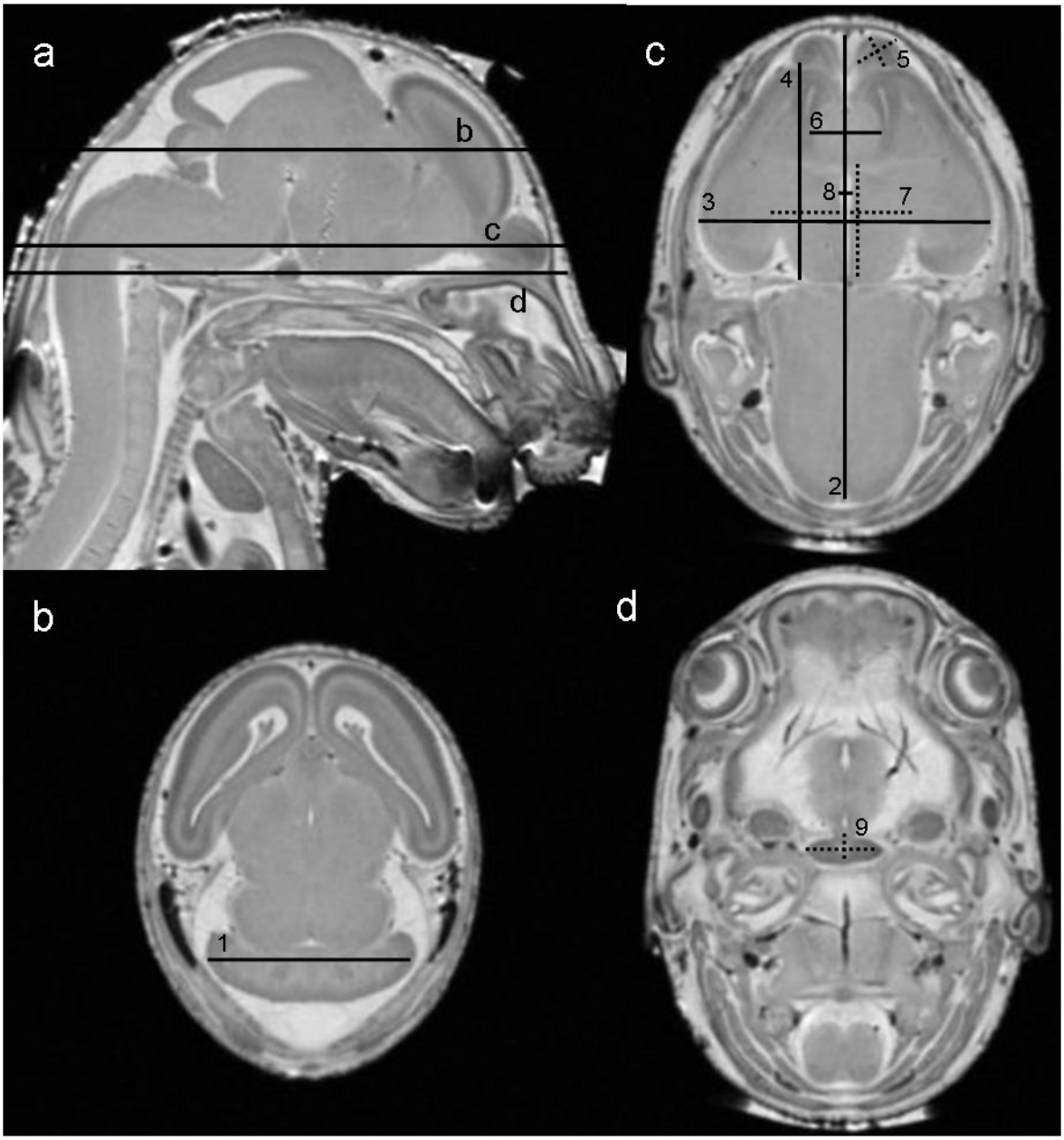

Figure 2.

MRM scans of GD17 fetuses allow for linear measurements of selected brain regions. Illustrated in (a) are the three different levels where measurements were attained as shown in b–d (b - at the widest point of the cerebellum; c – at the level of the anterior commissure; d – at the widest level of the pituitary gland). Dotted lines indicate that both length and width measurements were taken for that particular region. (1 = transverse cerebellar diameter, 2 = midsagittal brain length, 3 = brain width, 4 = frontothalamic distance, 5 = olfactory bulb length and width, 6 = septal region width, 7 = diencephalon length and width, 8 = 3rd ventricle width, 9 = pituitary length and width).

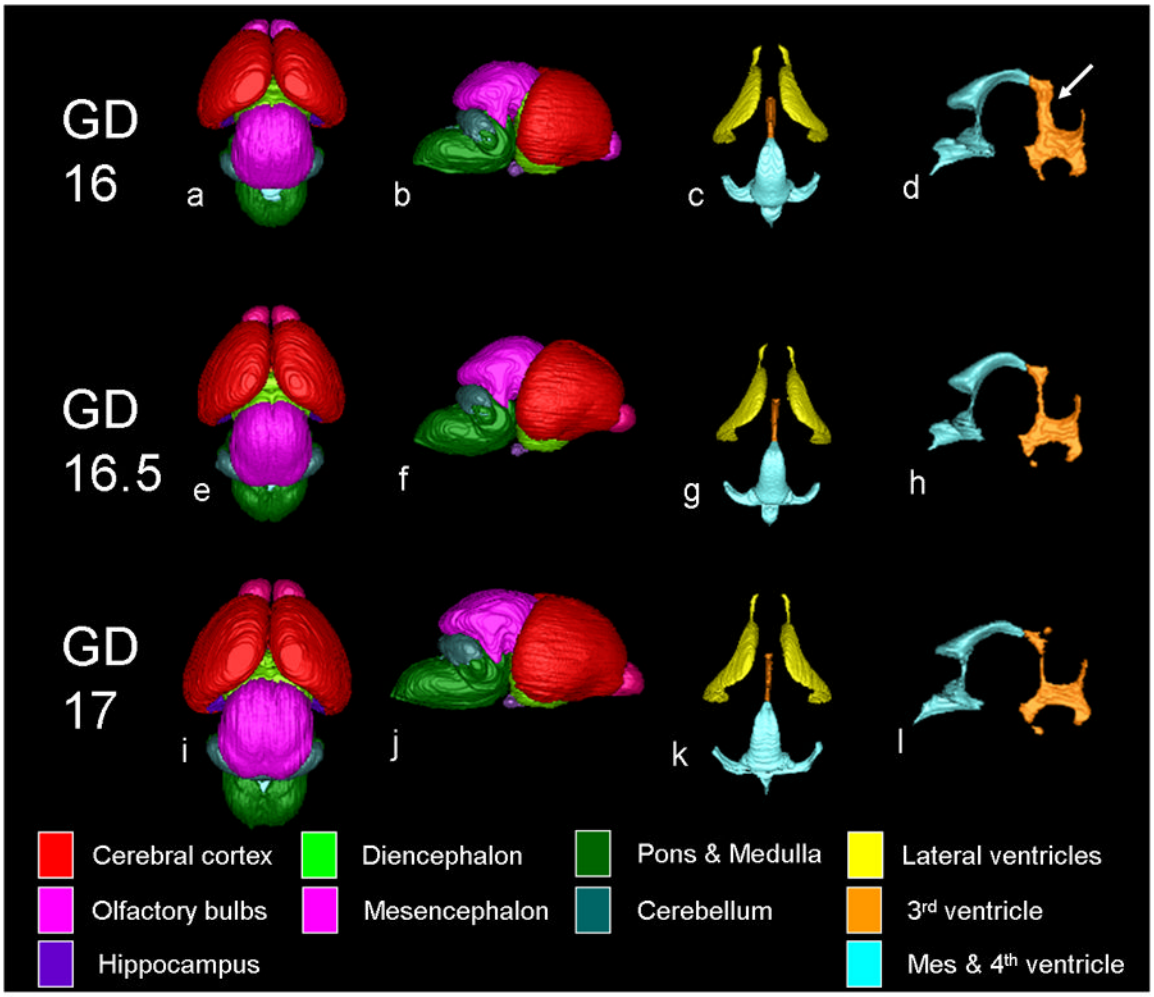

Figure 3.

Shown are 3D reconstructions of control GD16, GD16.5 and GD17 brains viewed from their dorsal (a, e, i) and lateral (b, f, j) aspects, as well as ventricular reconstructions as viewed from the dorsal side (c, g, k) and 3rd and mesencephalic & 4th ventricle reconstructions as seen from their lateral perspective (d, h, l). During development, brain regions increase in volume. The changing morphology of the olfactory bulbs is particularly evident. In contrast to the normal age-related increasing brain volumes, ventricular size decreases as a proportion of overall brain size with age (c & d, g & h, k & l). For the 3rd ventricle and mesencephalic & 4th ventricle, changes are particularly pronounced in the lateral MRM reconstructions (d, h, l). Note the thicker (wider) dorsal portion of the 3rd ventricle in GD16 (arrow in d) compared to GD16.5 (h) and GD17 (l) controls.

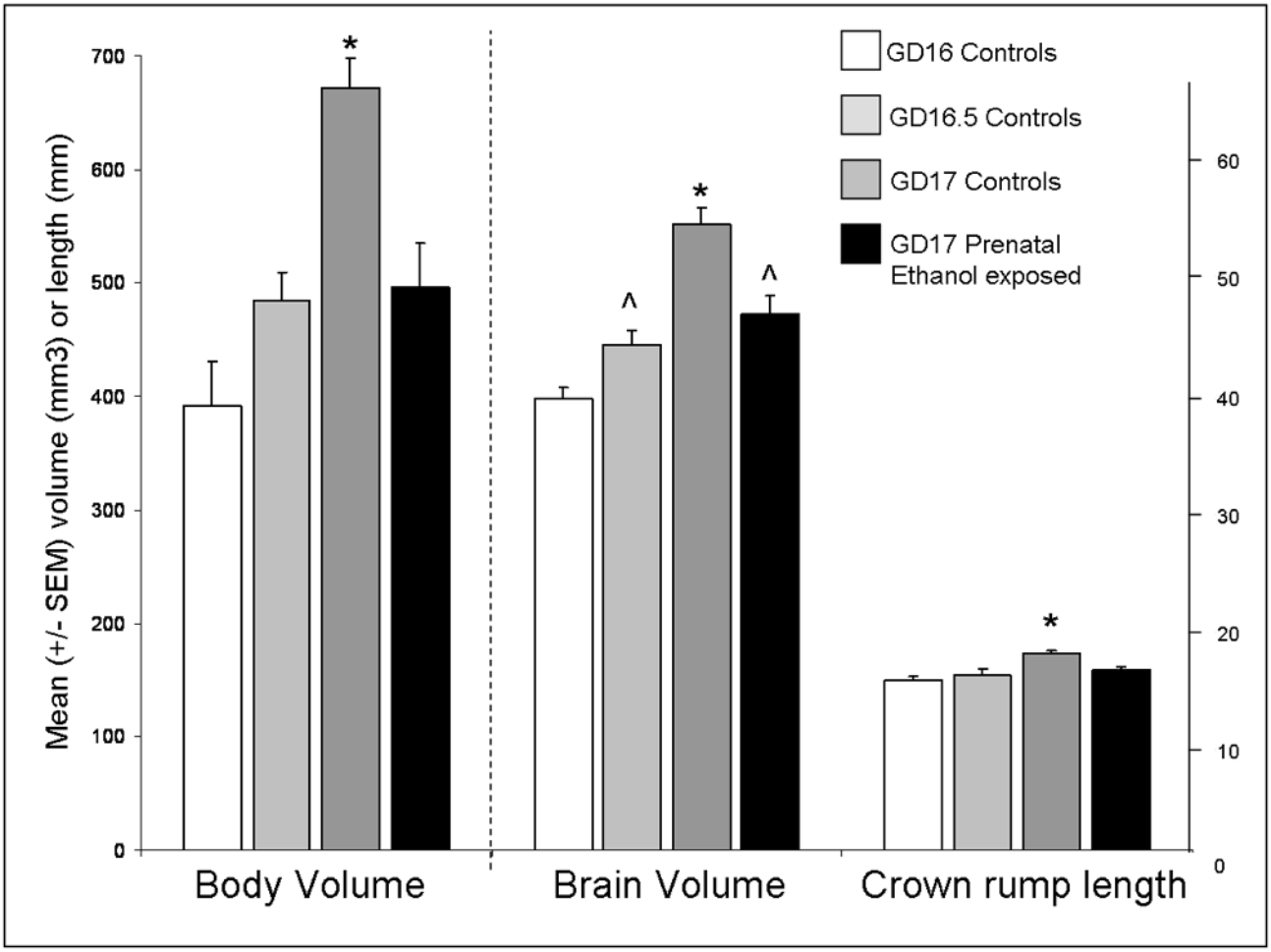

Figure 4.

Mean (± SEM) total body volume (mm^3), total brain volume (mm^3) and crown-rump length (CRL; mm) of the three control groups as well as in the prenatal ethanol-exposed subjects are reported. GD17 controls had significantly larger total body volumes and CRL as compared to all other groups ($p < 0.05$). Significant changes in total brain volume were also apparent at this time. * Significantly larger as compared to all other groups, $p < 0.05$; ^ significantly larger as compared to GD 16 controls only, $p < 0.05$.

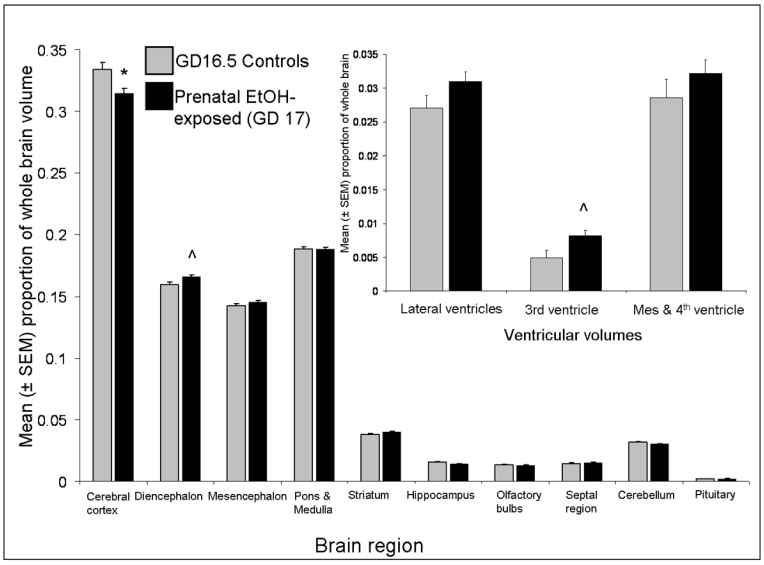

Figure 5.

Mean (± SEM) regional brain volumes expressed as a proportion of total brain volume in ethanol exposed and morphologically-comparable GD16.5 controls fetuses. Ethanol significantly decreased cortical volumes while increasing the volume of the diencephalon. The volume of the3rd ventricle was significantly increased after prenatal ethanol exposure. * Significantly decreased as compared to controls, $p < 0.05$; ^ significantly increased as compared to controls, $p < 0.05$.

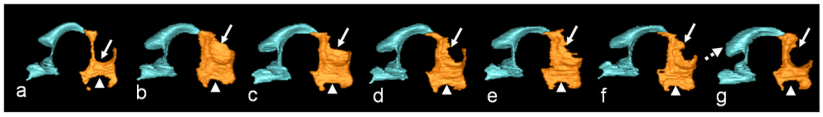

Figure 6.

GD10 ethanol exposure causes significant dysmorphology of the 3rd and mesencephalic & 4th ventricles. As compared to the normal appearance of the morphologically-matched control ventricles shown in a, the reconstructed ventricles from 6 out of 9 ethanol-exposed fetuses were dysmorphic (b-g). The 3rd ventricles appear to be too wide, involving those regions normally surrounded by the thalamus (arrows) and hypothalamus (arrowheads) (b – g). In addition, a considerable expansion of the mesencephalic ventricle is evident in g (dashed arrow).

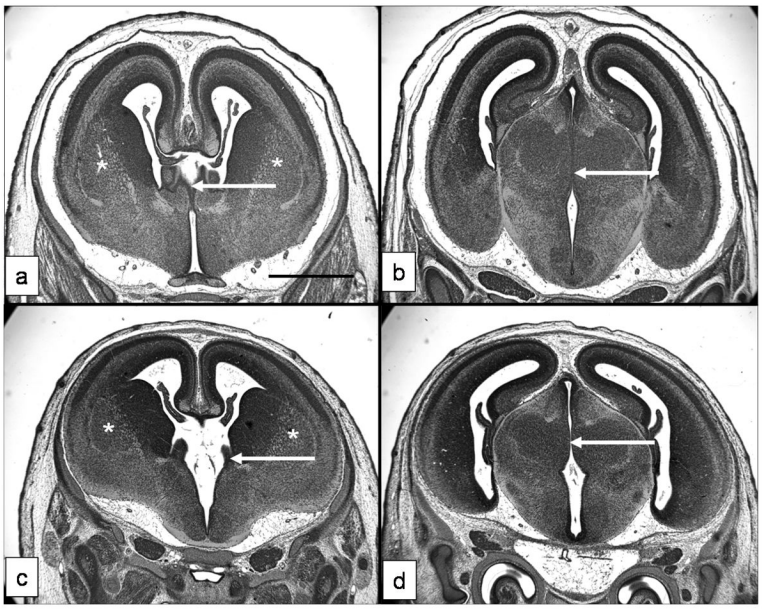

Figure 7.

Histological H&E-stained coronal sections illustrate corresponding points in the brain of a GD16.5 control (a, b) and a GD17 ethanol-exposed (c, d) fetus. Sections through the rostral part of the 3rd ventricles (a, c; arrows) at a point where the lateral ventricles and striatum (*) are also clearly evident, show considerable dilation of the 3rd ventricle in the ethanol-exposed subject. This is also apparent at a more caudal level (b and d), where, as opposed to the normal midline apposition of the thalamic (arrow in b) tissue, in the ethanol-exposed animal (d) the space of the 3rd ventricle is clearly evident (arrow in d). Bar = 0.5 mm

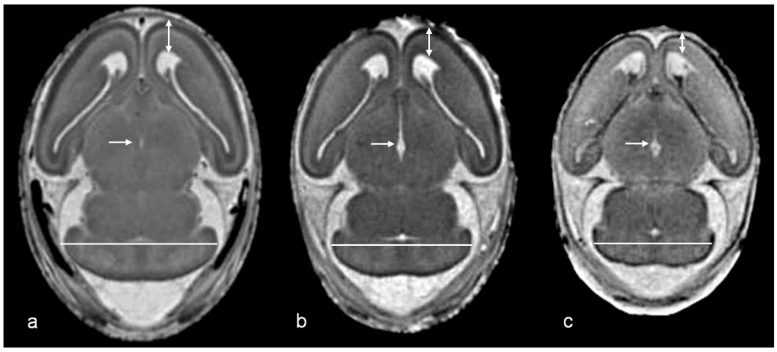

Figure 8.

Comparison of horizontal MRM scans from a GD16.5 control (a) and two GD17 ethanol-exposed fetuses (b & c) illustrates enlargement of the 3rd ventricles (arrows) and reduced thickness of the cerebral cortex (double-sided arrows). Mild cortical reduction is apparent in b, while it is more obvious in c. Also notable is an excess of choroid plexus in the lateral ventricle and reduced transverse cerebellar diameter (line) in the ethanol-exposed subject pictured in (c). Bar = 1 mm.

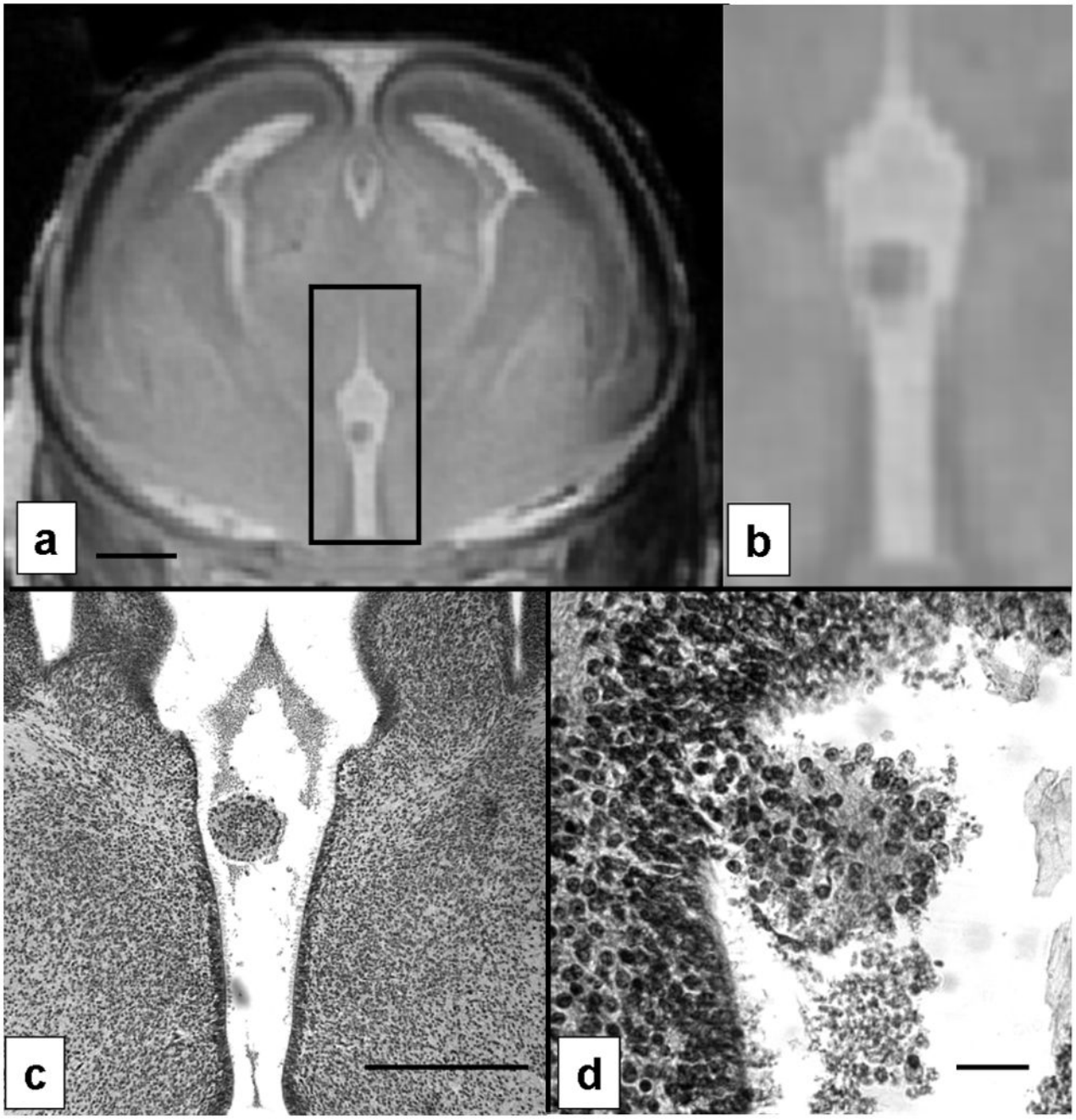

Figure 9.
MRM images (a, b) and H&E-stained histological sections (c & d) from an ethanol-exposed subject illustrate a heterotopic mass extending into the 3rd ventricle. Sequential histological sections illustrated the hypothalamic point of origin and neural nature of the heterotopia. Bar in: a = 0.5 mm; c = 0.5 mm; d = 0.25 mm.

Birth Defects Res A Clin Mol Teratol. Author manuscript; available in PMC 2012 September 18.

Table 1

Regional brain volumes in GD16, GD16.5 and GD17 control and ethanol-exposed mice
Volumetric data for brains of control and ethanol-exposed fetuses.

Brain volumes (mm3)	**Controls**				**Ethanol-exposed**	
Region	**GD16**	**GD16.5**	**GD17**	**Developmental trend**	**GD 17**	**vs GD16.5 controls**
Cerebral cortex	12.99 ± 0.43	14.87 ± 0.43	18.51 ± 0.59	*	14.90 ± 0.73	
Diencephalon	6.26 ± 0.13	7.11 ± 0.20	8.89 ± 0.22	*	7.83 ± 0.27	
Mesencephalon	5.52 ± 0.21	6.34 ± 0.24	7.71 ± 0.20	*	6.84 ± 0.21	
Pons & Medulla	7.46 ± 0.17	8.38 ± 0.33	10.51 ± 0.36	*	8.89 ± 0.31	
Striatum	1.38 ± 0.05	1.69 ± 0.09	2.19 ± 0.10	*	1.88 ± 0.07	
Hippocampus	0.58 ± 0.03	0.70 ± 0.04	0.96 ± 0.07	^	0.68 ± 0.04	
Olfactory bulbs	0.43 ± 0.04	0.60 ± 0.03	0.87 ± 0.05	*	0.62 ± 0.04	
Septal region	0.57 ± 0.01	0.65 ± 0.02	0.88 ± 0.04	*	0.72 ± 0.03	
Cerebellum	1.23 ± 0.02	1.40 ± 0.05	1.71 ± 0.08	^	1.43 ± 0.06	
Pituitary	0.10 ± 0.03	0.09 ± 0.00	0.11 ± 0.00	^	0.11 ± 0.00	*
Lateral ventricles	1.40 ± 0.08	1.20 ± 0.03	1.28 ± 0.06		1.45 ± 0.04	*
Third ventricle	0.37 ± 0.02	0.22 ± 0.02	0.21 ± 0.02	#	0.38 ± 0.04	*
Mes & 4th ventricle	1.56 ± 0.05	1.27 ± 0.07	1.31 ± 0.08	#	1.49 ± 0.07	

Data are reported in mm^3 and are presented as the mean ± SEM. Significant developmental trends are indicated with the following symbols:

*regional brain volumes of the GD16.5 and GD17 controls are significantly larger as compared to the GD16 controls and volumes of the GD17 controls are significantly larger as compared to GD16.5 controls;

^regional brain volumes of the GD17 controls are significantly larger as compared to the GD16 and GD16.5 controls, but the GD16 and GD16.5 controls do not differ;

#ventricular volumes of the GD16 controls are significantly larger as compared to those of the GD16.5 and GD17 controls, the GD16.5 and GD17 control volumes do not differ; all p's < 0.05.

Data from ethanol-exposed fetuses is also illustrated. Note that as compared to the GD17 controls, regional brain volumes tend to be reduced while ventricular volumes are increased after prenatal ethanol and that the means most closely approximate the GD16.5 controls'. As compared to the GD16.5 controls, prenatal ethanol-exposed animals had larger pituitary, lateral and 3rd ventricular volumes (* p < 0.05).

Birth Defects Res A Clin Mol Teratol. Author manuscript; available in PMC 2012 September 18.

Table 2

Brain linear measurements in GD16, GD16.5 and GD17 control and ethanol-exposed mice
Linear brain measurement data in control and ethanol-exposed fetuses.

Brain linear measurements (mm)	**Controls**				**EtOH-exposed**	
Measurement	**GD16**	**GD16.5**	**GD17**	**Developmental trend**	**GD17**	**vs GD16.5 controls**
Mid-sagittal brain length	6.57 ± 0.07	7.00 ± 0.09	7.56 ± 0.06	*	7.15 ± 0.12	
Cortical brain width	4.21 ± 0.03	4.27 ± 0.06	4.68 ± 0.06	^	4.38 ± 0.09	
Frontothalamic distance	3.31 ± 0.03	3.64 ± 0.06	4.02 ± 0.04	*	3.71 ± 0.09	
Transverse cerebellar diameter	2.93 ± 0.04	3.20 ± 0.06	3.47 ± 0.05	*	3.25 ± 0.07	
Olfactory bulb length (avg. right and left)	0.40 ± 0.02	0.46 ± 0.03	0.57 ± 0.02	^	0.43 ± 0.03	
Olfactory bulb width (avg. right and left)	0.61 ± 0.02	0.64 ± 0.04	0.74 ± 0.02	^	0.63 ± 0.02	
Septal region width	1.07 ± 0.02	1.08 ± 0.01	1.16 ± 0.01	^	1.14 ± 0.01	*
Diencephalon						
Length	1.58 ± 0.01	1.72 ± 0.05	1.91 ± 0.03	*	1.75 ± 0.03	
Width	1.96 ± 0.01	1.97 ± 0.03	2.12 ± 0.03	^	2.03 ± 0.02	
Pituitary gland						
Length	0.35 ± 0.01	0.35 ± 0.01	0.38 ± 0.01		0.41 ± 0.01	*
Width	1.08 ± 0.03	1.04 ± 0.03	1.17 ± 0.03	^	1.08 ± 0.03	
3rd ventricle width	0.30 ± 0.02	0.24 ± 0.01	0.21 ± 0.01	#	0.35 ± 0.02	*

Data are reported in mm and are presented as the mean ± SEM. Significant developmental trends are indicated with the following symbols:

* linear measurements of the GD16.5 and GD17 controls are significantly larger as compared to GD16 controls and volumes of the GD17 controls are significantly larger as compared to GD16.5 controls;

^ linear measures of the GD17 controls are significantly larger as compared to the GD16 and GD16.5 controls, but the GD16 and GD16.5 controls do not differ;

ventricular measures of the GD16 controls are significantly larger as compared to the GD16.5 and GD17 controls, the GD16.5 and GD17 control volumes do not differ; all p's < 0.05.

Data from ethanol-exposed fetuses is also illustrated. As compared to the GD16.5 controls, septal region width, pituitary gland length and third ventricle width is significantly larger in subjects exposed to ethanol prenatally (* $p < 0.05$).